Onset of Void Coalescence during Dynamic Fracture of Ductile Metals

E. T. Seppälä, J. Belak, and R. E. Rudd

Lawrence Livermore National Laboratory, Condensed Matter Physics Division, L-415, Livermore, California 94551, USA

(Received 3 June 2004; published 10 December 2004)

Molecular dynamics simulations in three-dimensional copper are performed to quantify the void coalescence process leading to fracture. The correlated growth of the voids during their linking is investigated both in terms of the onset of coalescence and the ensuing dynamical interactions through the rate of reduction of the distance between the voids and the directional growth of the voids. The critical intervoid ligament distance marking the onset of coalescence is shown to be approximately one void radius in both measures.

DOI: 10.1103/PhysRevLett.93.245503 PACS numbers: 61.72.Qq, 61.72.Lk, 62.20.Fe, 62.20.Mk

The point at which voids begin to coalesce during dynamic fracture is of considerable interest because complete fracture of the material typically ensues rapidly thereafter. A robust model of the onset of coalescence is an important ingredient of a predictive model of dynamic fracture. The conventional picture of how ductile metals break under the rapid application of stress consists of three stages: void nucleation, growth, and coalescence. Initially voids nucleate from the weak points in the material such as inclusions and/or grain boundary junctions. Once nucleated, the voids grow under the tensile stress, driven by the reduction in elastic energy. Eventually, the voids grow sufficiently large that they interact with each other, coalesce into larger voids, and finally form the fracture surface [1,2]. There are many interesting twists and subtleties, such as the interplay between shear localization and void growth, but the basic picture applies to the fracture of a broad class of ductile metals. Naturally considerable effort has gone into the study of this fracture process, both in modeling and theory and in experiment, including a new generation of 3D, nondestructive fracture characterization techniques such as x-ray tomography. Nevertheless, a robust, mechanistic understanding of coalescence has yet to emerge.

Computationally void growth has been studied extensively at the continuum level, [3–6] and more recently at the atomistic level [7–9]. The atomistic studies demonstrate that voids grow by emitting dislocations, which carry away the material, platelets of atoms, from the void and are responsible for the plastic deformations needed to accommodate significant void growth. There are also many recent studies of fracture in ductile metals with several holes or voids [10]. While these studies model the void growth explicitly, often with fairly sophisticated models of plasticity, they typically simplify the coalescence process to instantaneous unification of the voids based on a relatively simple criterion such as growth of the voids to within one void diameter of each other or a plastic strain threshold. The earlier continuum studies (cf., Ref. [6]), and the one atomistic study known to us [11] of the coalescence process have been conducted in effectively two-dimensional and highly symmetric systems.

In this Letter we analyze the details of the onset of void coalescence. In particular we quantify the point at which coalescence begins, as measured by a critical *intervoid ligament distance* (ILD), and examine the mechanisms involved in the transition from independent void growth to coalescence. There are several ways in which two voids can interact. In the case of pure impingement, the voids only interact when they grow to the point that they intersect and join into a single void. In reality, the voids interact before they intersect. Their range of interaction is extended due to their elastic and plastic fields. Each void generates an elastic strain field of the form associated with centers of dilatation [12], with a shear stress that decreases with the distance like r^{-3}. For voids sufficiently close, each void's growth rate is altered by the stress field of the proximal void. The modification of the elastic field can affect the initiation of plasticity, as well as the subsequent development of the plastic zone around the voids. The voids may interact through their plastic fields, too, in which case the fields may give rise to an increased hardening rate in a localized region or to thermal softening and shear localization. An argument due to Brown and Embury for a transition to shear deformation based on simple geometrical considerations suggests that the critical intervoid ligament distance, ILD_c, should be equal to one diameter of a void [13]; that is, when the surfaces of a pair of voids are separated by one void diameter, they transition from independent void growth to coalescence. It is at this point, they argue, that the dominant void process switches from the radial plastic flow around isolated growing voids to a shear deformation allowing the rapid coalescence of the pair of voids. However, more recent two-dimensional studies suggest that for distances between voids as large as six diameters the void growth rate is enhanced [14].

The use of atomistic techniques permits the analysis of the contributions of these competing mechanisms to the onset of void coalescence, as we describe in this Letter. We demonstrate the existence of, and compute, the criti-

cal intervoid ligament distance ILD_c by starting with two voids well separated from each other and detecting the point at which correlated growth begins, marked both by the accelerated rate at which the two-void surfaces approach each other and by biased growth causing the voids to start to extend toward each other. This gives an indication of the onset of the coalescence process, and it tests the argument by Brown and Embury [13]. We also test the setup by Horstemeyer *et al.* [14] by varying the initial distances between the voids and measuring the asymptotic growth rate of the voids.

We have performed large-scale (parallel) classical molecular dynamics (MD) simulations [15] in single crystal face-centered cubic (fcc) systems using an empirical embedded-atom model potential for copper [16]. The three-dimensional (3D) simulation box consists of $120 \times 120 \times 120$ 4-atom fcc unit cells with periodic boundary conditions for a total of 6 912 000 atoms. The system is initially equilibrated using a thermostat [17] at $T = 300$ K and a constant volume L^3 (with $L = 43.4$ nm) chosen to give ambient pressure, $P \simeq 0$ MPa. Once the system has reached equilibrium, two spherical voids are cut in the system with radius $r_0 = 0.05L = 2.2$ nm: one in the middle of the box and the other 12.2 nm away, in a relative position of $[0.25, 0.1166, 0.0544]L$. We refer to these as void A and void B, respectively, see Fig. 1. When the initial distance between the voids is varied, the location of the void B is changed, but the relative orientation of the voids is kept fixed. Initially, the voids are equal in size, with approximately 3620 atoms removed for each. Once the voids are formed, the thermostat is turned off, and dilatational strain is applied uniformly at a constant strain rate $\dot{\varepsilon}$. Applied strain rates of $\dot{\varepsilon} = 10^8/\mathrm{s}$ and $10^9/\mathrm{s}$

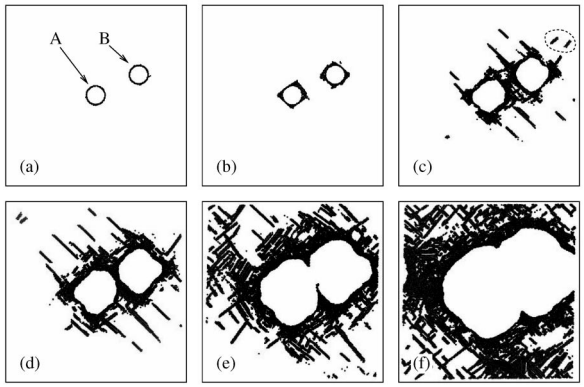

FIG. 1. Snapshots of the slices of the two-void system at $\dot{\varepsilon} = 10^9/\mathrm{s}$ with only those atoms shown that are in dislocation cores, stacking faults, void surfaces, or other defects (see text). The dashed loop in panel (c) is drawn around a slice of a prismatic dislocation loop. The plane shown passes through the centers of both voids. The snapshots show the initial plasticity (a),(b), interacting plastic zones (c),(d), and the final coalescence (e),(f). The frames correspond to strains of $\varepsilon = 1.72\%$, 2.42%, 3.47%, 3.89%, 4.52%, and 5.21%, respectively.

have been used with perfectly triaxial, or hydrostatic, expansion. The dilatation is simulated by expanding the simulation box at each time step [7], as in the Parrinello and Rahman technique [18]. More details about the simulation methods are in Ref. [9].

While some void growth takes place through elastic stretching in the initial phases of the box expansion, significant void growth and void-void interaction take place only once plastic deformation has begun. The important role of plasticity forces us to consider in some detail how dislocations are generated and the effect the dislocation dynamics have on void coalescence. Figure 1 shows a visualization within a slice of width 4.5 Å of a plane including centers of both voids at six different instants during coalescence. The atoms shown are either on the surface of the voids or belong to dislocations. The decision of which atoms to plot is based on a geometrical criterion, a finite-temperature generalization of the centrosymmetry deviation [8,19]. From the snapshots one sees that the deformation mechanism involves the nucleation and propagation of dislocations, accommodating the void growth, and the interaction of the dislocations. For example, the prismatic dislocation loops punched out by the voids appear as roughly parallel line traces (due to the stacking fault ribbons) in the slice Fig. 1(c), as verified in the full 3D configuration. Initially the dislocation activity around each void is essentially symmetric [Fig. 1(a) and 1(b)], as expected for independent void growth, but as the plastic fields evolve the void-void interaction is clearly evident both through interactions between the two plastic zones and bias due to the elastic fields [Fig. 1(c)]. Once the dislocation density grows sufficiently high in the ligament region between the voids [Figs. 1(d)], void B begins to grow in the direction away from void A. Eventually the voids coalesce [Fig. 1(e)], and continue to grow as one until coalescence with the void's periodic images takes place [subsequent to Fig. 1(f)] and the cavity percolates through the periodic system.

Figure 1 offers several visual indications of the interaction between voids. Clearly, the separation between the void surfaces (the ILD) serves as something akin to a reaction coordinate for the coalescence: the voids coalesce when it goes to zero. In Fig. 2 the dynamic evolution of the ILD has been plotted for strain rates $\dot{\varepsilon} = 10^8/\mathrm{s}$ and $10^9/\mathrm{s}$ and for various *initial* closest surface-to-surface distances between the voids ILD_0. In Fig. 1 the case $\mathrm{ILD}_0 \simeq 1.8$ was shown. While the strain is the quantity controlled in these simulations, we have found that the data collapse well and the coalescence is indicated much more clearly if the ILD data are plotted as a function of the linear mean void size, $\bar{f}^{1/3}$, where $\bar{f}$ is the average of the two-void fractions $f = V_{\mathrm{void}}/V$ and V is the volume of the box. The technique for calculating the void volume is described in Ref. [9]. The reason is that for voids growing independently, the ILD is closely related to

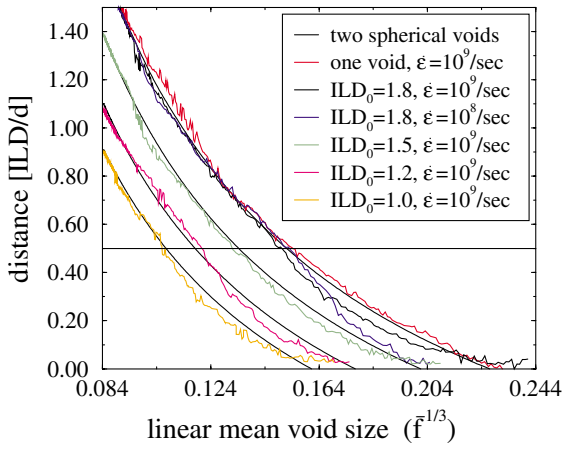

FIG. 2 (color). The dynamical ILD, the distance between the surfaces of the voids along the line connecting the original center positions, plotted versus the mean void size $\bar{f}^{1/3}$ for various initial ILD_0's. The ILD is plotted in units of the average void diameter d calculated at each instant using the formula $d = 2[3/(4\pi)\bar{f}V]^{1/3}$, assuming roughly spherical voids. For reference, thin lines are plotted to show the relationship for spherical voids impinging freely on each other (see text). The red line shows the hypothetical ILD computed by duplicating the single void at fixed centers with $\mathrm{ILD}_0 = 1.8$. The horizontal line is at $\mathrm{ILD} = 0.5d$.

the size of the void through geometry. In particular, the ILD for two spherical voids of the same diameter d growing independently is given by $\mathrm{ILD} = (\mathrm{ILD}_0 + d_0) \times (1 + \varepsilon) - d$, where d_0 is the initial diameter. This formula is used to generate the thin curves in Fig. 2. Deviations from these free impingement curves in the MD simulations indicate void shape changes, most importantly anisotropic growth due to coalescence. The same data plotted versus strain exhibit a strong strain-rate dependence inherited from the void growth law $V_{\mathrm{void}}(\varepsilon)$ (cf., Ref. [9]). For reference, the snapshots in Fig. 1(a)–1(d) correspond to mean linear void size $\bar{f}^{1/3} = 0.089$, 0.094, 0.150, and 0.195, respectively. After coalescence $\bar{f}$ is not calculated.

Initially the separation distance decreases essentially smoothly until the plasticity begins, eventually reaching zero. A transition occurs when the ILD starts to decrease much faster than the free impingement line, which takes place when the ILD reaches approximately one half: $\mathrm{ILD}_c = 0.5 \pm 0.1$ diameter or one radius, independently of ILD_0 or the strain rate. Note that the unit of ILD is the current diameter of a void, d, not the initial value. A curve derived from a single void growth is provided to estimate the contribution of uncorrelated faceting effects (the "one void" curve at $\mathrm{ILD}_0 = 1.8$), and these effects are seen to be relatively small. The critical ILD of one radius is much lower than the Brown-Embury estimate, and it corresponds to a strain of 3.47% ($\bar{f}^{1/3} \simeq 0.15$) for $\mathrm{ILD}_0 = 1.8$ at $\dot{\varepsilon} = 10^9/\mathrm{s}$, corresponding to Fig. 1(c). In the very final stages the ligament is drawn under biaxial stress, and the flow switches from radial material transport to tangential transport as the mechanism switches from loop punching to drawing. At this point, the material is highly defective but it remains ductile. There is no abrupt fracture, as might be expected at larger length scales. Coalescence results from extended drawing and thinning of the ligament until rupture.

Another measure of void interactions is whether the voids grow preferentially toward their neighbor. This effect is quantified in Fig. 3, which shows the motion of the center of mass of the void surface (the void center) for the voids shown in Fig. 1. Here $\mathrm{ILD}_0 = 1.8$ and $\dot{\varepsilon} = 10^9/\mathrm{s}$. After the void growth starts, the center of void A initially moves only slightly, but at about $\bar{f}^{1/3} = 0.15$ ($\mathrm{ILD} = 0.5$ in Fig. 2), it starts to move in the direction of the other void as the void growth becomes biased toward its neighbor. Just before coalescence the center of void A begins to move away from void B, as the growth is biased in the opposite direction. During this sequence, void B initially grows away from void A, then roughly in unison with void A ($\bar{f}^{1/3} = 0.15$) it begins to grow toward its neighbor, and before coalescence it too switches to growth away from the proximal void. This retrograde growth happens at the same point (after $\bar{f}^{1/3} = 0.19$) as the decrease of ILD begins to slow down in Fig. 2 [see also the snapshot in Fig. 1(d)]. The same phenomenon—first slow movement or repulsion from the void; then growth toward the nearby void after $\bar{f}^{1/3} = 0.15$ ($\mathrm{ILD} = 0.5$); and finally retrograde growth—holds in the $\dot{\varepsilon} = 10^8/\mathrm{s}$ case, too, in Fig. 3. As a reference, the movement

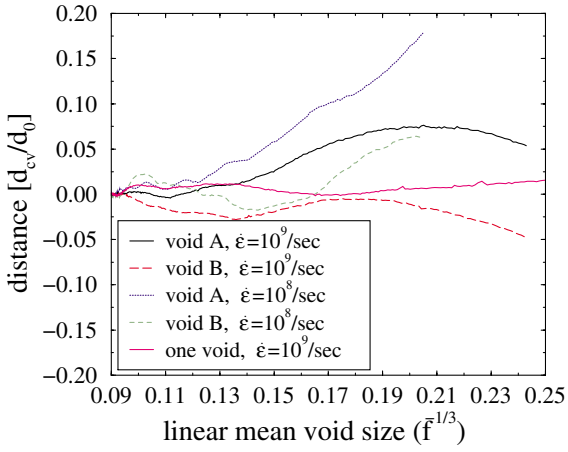

FIG. 3 (color online). Distance d_{cv} from the original center of void to the instantaneous void center, projected onto the line connecting the original void centers, plotted versus the average void size to the point of coalescence ($\mathrm{ILD} \simeq 0$). The sign of the distance d_{cv} is positive for motion toward the other void. $\mathrm{ILD}_0 = 1.8$. The thin solid line is for a single void in the same size of the box and with the same radius and $\dot{\varepsilon} = 10^9/\mathrm{s}$ projected to the same line. Here the distance d_{cv} is given in the units of the original void diameter d_0.

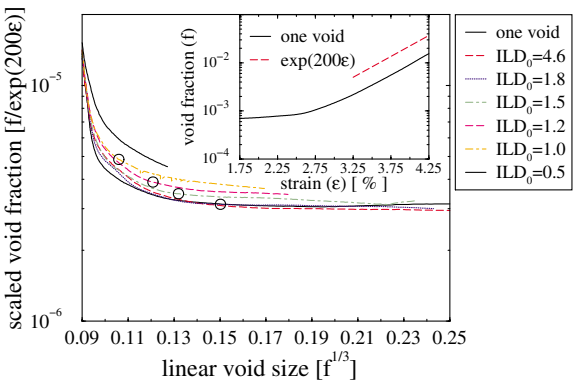

FIG. 4 (color online). Growth of the voids until coalescence presented by void fraction for $\mathrm{ILD}_0 = 0.5, 1.0, 1.2, 1.5, 1.8$, and 4.6 diameters as well as in a single void case (in the same box size) at $\dot{\epsilon} = 10^9/\mathrm{s}$. The asymptotic behavior (before finite size effects) is exponential growth with $\exp(200\epsilon)$ as seen in the inset for the single void case. In the main figure the void fraction f has been scaled with the exponential. The circles point to where the dynamical ILD's cross the line ILD = 0.5 in Fig. 2.

of the center of a single void in a box with $\dot{\epsilon} = 10^9/\mathrm{s}$ projected to the same line is plotted. Comparing the single void case with the interacting voids, one sees that the maximum distance the centers of the interacting voids have moved is 3 to 5 times larger than the nanoscale random walk of the single void, and not just due to statistical fluctuations at the void surface.

We have identified the onset of coalescence, but it is also interesting to examine the subsequent void growth prior to coalescence. How does this differ from the exponential growth of an isolated void [7,9]? In order to analyze the correlated growth, we have factored out the noninteracting growth rate, $\exp(200\epsilon)$, from f in the plot in Fig. 4. The factor of 200 in the exponential is derived from the single void case, as indicated in the inset of the figure. The void growth data for $\mathrm{ILD}_0 = 4.6$ and 1.8 coincide with the single void curve. The void growth rate with smaller ILD_0's reach their asymptotic growth rate earlier. As can be seen from the figure, there is no marked change in the void volume behavior at the point when the voids start to interact (indicated by the circles).

We have also performed a series of simulations of a fixed void in varying box size in order to find the coalescence process of the void with its (six) periodic image(s), similar to the manner in which some continuum calculations of coalescence have been done. The details will be reported elsewhere [20], but it is worth noting, that the behavior is opposite to the results above in an important way. The smaller the box size, and hence the smaller the ILD, the later the void starts to grow.

To summarize, interaction and coalescence of two voids in copper under tension were studied with multi-million-atom MD simulations. The effect of interactions between voids has been quantified by the increased reduction-rate of their separation and the movement of their centers. The critical intervoid ligament distance has been found to be close to 1 void radius, independent of the strain rate or the starting separation ILD_0, when the plastic zones surrounding the voids first interact strongly.

This work was performed under the auspices of the U.S. Department of Energy by the Univ. of Cal., Lawrence Livermore National Laboratory, under Contract No. W-7405-Eng-48.

[1] D. R. Curran, L. Seaman, and D. A. Shockey, Phys. Rep. **147**, 253 (1987).
[2] F. A. McClintock, in *Metallurgical Effects at High Strain Rates*, edited by R.W. Rhode, B. M. Butcher, and J. R. Holland (Plenum, New York, 1973).
[3] F. A. McClintock, J. Appl. Mech. **6**, 363 (1968).
[4] J. R. Rice and D. M. Tracey, J. Mech. Phys. Solids **17**, 201 (1969).
[5] A. L. Gurson, J. Eng. Mater. Technol. **99**, 2 (1977).
[6] J. Koplik and A. Needleman, Int. J. Solids Struct. **24**, 835 (1988).
[7] J. Belak, in *Shock Compression of Condensed Matter*, edited by S. C. Schmidt *et al.* (American Institute of Physics, New York, 1997).
[8] R. E. Rudd and J. Belak, Comput. Mater. Sci. **24**, 148 (2002).
[9] E. T. Seppälä, J. Belak, and R. E. Rudd, Phys. Rev. B **69**, 134101 (2004).
[10] J. P. Bandstra and D. A. Koss, Mater. Sci. Eng. A **319-321**, 490 (2001); A. B. Geltmacher, D. A. Koss, P. Matic, and M. G. Stout, Acta Mater. **44**, 2201 (1996); P. E. Magnusen, D. J. Srolovitz, and D. A. Koss, Acta Metall. Mater. **38**, 1013 (1990); P. E. Magnusen, E. M. Dubensky, and D. A. Koss, Acta Metall. **36**, 1503 (1988); V. Jablokov, D. M. Goto, and D. A. Koss, Metall. Mater. Trans. A **32**, 2985 (2001).
[11] B. P. Somerday, P. D. Pattillo II, M. F. Horstemeyer, and M. I. Baskes, Mater. Res. Soc. Symp. Proc. **578**, 333 (2000).
[12] J. D. Eshelby, Proc. R. Soc. London A **252**, 561 (1959).
[13] L. M. Brown and J. D. Embury, in *Proceedings of the Third International Conference on Strength of Metals and Alloys* (Institute of Metals, London, 1973).
[14] M. F. Horstemeyer, M. M. Matalanis, A. M. Sieber, M. L. Botos, International Journal of Plasticity **16**, 979 (2000).
[15] M. P. Allen and D. J. Tildesley, *Computer Simulations of Liquids* (Oxford University, Oxford, 1987).
[16] D. J. Oh and R. A. Johnson, J. Mater. Res. **3**, 471 (1988).
[17] W. G. Hoover, Phys. Rev. A **31**, 1695 (1985).
[18] M. Parrinello and A. Rahman, J. Appl. Phys. **52**, 7182 (1981).
[19] C. L. Kelchner, S. J. Plimpton, and J. C. Hamilton, Phys. Rev. B **58**, 11085 (1998).
[20] E. T. Seppälä, J. Belak, and R. E. Rudd (unpublished).